

The rate of granule ripple movement on Earth and Mars

James R. Zimbelman^{a,*}, Rossman P. Irwin III^a, Steven H. Williams^b, Fred Bunch^c,
Andrew Valdez^c, Scott Stevens^d

^a Center for Earth and Planetary Studies, National Air and Space Museum MRC 315, Smithsonian Institution, Washington, DC 20013-7012, USA

^b Education Division, National Air and Space Museum MRC 305, Smithsonian Institution, Washington, DC 20013-7012, USA

^c Great Sand Dunes National Park and Preserve, 11500 Highway 150, Mosca, CO 81146-9798, USA

^d National Climatic Data Center, Federal Building, 151 Patton Ave., Asheville, NC 28801-5001, USA

ARTICLE INFO

Article history:

Received 25 July 2008

Revised 13 March 2009

Accepted 13 March 2009

Available online 17 April 2009

Keywords:

Earth

Geological processes

Mars surface

ABSTRACT

The rate of movement for 3- and 10-cm-high granule ripples was documented in September of 2006 at Great Sand Dunes National Park and Preserve during a particularly strong wind event. Impact creep induced by saltating sand caused ~ 24 granules min^{-1} to cross each cm of crest length during wind that averaged $\sim 9 \text{ m s}^{-1}$ (at a height well above 1 m), which is substantially larger than the threshold for saltation of sand. Extension of this documented granule movement rate to Mars suggests that a 25-cm-high granule ripple should require from hundreds to thousands of Earth-years to move 1 cm under present atmospheric conditions.

Published by Elsevier Inc.

1. Introduction

Granule ripples are aeolian bedforms comprised of a sandy core that is covered by a surface layer of granules, particles that are typically 1–2 mm in diameter (e.g., Bagnold, 1941, pp.154–156; Sharp, 1963; Ellwood et al., 1975; Fryberger et al., 1992). Several names have been applied to these features in the literature, but here we use ‘granule ripple’ to represent all wind-generated bedforms that are coated by granule-sized particles. Granule ripples are significantly larger than wind ripples formed in well-sorted fine sand, yet they are generally smaller than an individual sand dune. Interest in granule ripples increased recently due to results from the Mars Exploration Rovers (MERs) Spirit and Opportunity, both of which documented the common occurrence of sand-cored ripples coated with granule-sized particles (Fig. 1; Greeley, 2004, 2006; Sullivan, 2005, 2008). No MER observations document movement of a martian granule ripple, although Spirit recently did document active sand ripple movement (Sullivan, 2008). The extensive literature regarding different proposed modes of formation of sand ripples is in marked contrast to the general agreement that granule ripples result from the creep of granule particles induced by the impact of saltating sand grains; the ‘armoring’ effect of the granules contributes directly to spectacular growth of both the height and wavelength of these features, as compared to typical sand rip-

ples. This report describes a documented rate of movement for granule ripples observed at Great Sand Dunes National Park and Preserve (GSDNPP) in south-central Colorado. The GSDNPP results are then used to make inferences about potential granule ripple movement under present conditions on Mars.

2. Background

Bagnold (1941) was the first person to present detailed measurements of how sand moves both in the natural environment and in the laboratory. He pointed out an important distinction between sand ripples, which he related to the motion of individual sand grains, and sand dunes, which he described as the result of the interaction of the cloud of saltating sand with the wind that drives the grains across the surface (Bagnold, 1941, pp. 149–153, 180–183). Sharp (1963) used field data from sites throughout the southwestern United States to argue that sand ripple wavelengths were more a function of the shadowing effect of the upstream ripple crest than the Bagnold view that sand ripple wavelength was a manifestation of the average saltation path length. Both the Bagnold and Sharp concepts of sand ripples have been explored with laboratory experiments and associated theory involving both reptation (a ‘crawling’ motion of the sand grains along the surface) and saltation (the ‘jumping’ motion of sand grains well above the surface). Splash caused by impacting sand grains produces surface variations that preferentially grow to form typical sand ripples (Anderson, 1987; Anderson and Haff, 1988, 1991; Anderson and Bunas, 1993). In spite of the controversy in understanding how

* Corresponding author. Address: CEPS/NASM MRC 315, Smithsonian Institution, Washington, DC 20013-7012, USA. Fax: +1 202 786 2566.

E-mail address: zimbelmanj@si.edu (J.R. Zimbelman).

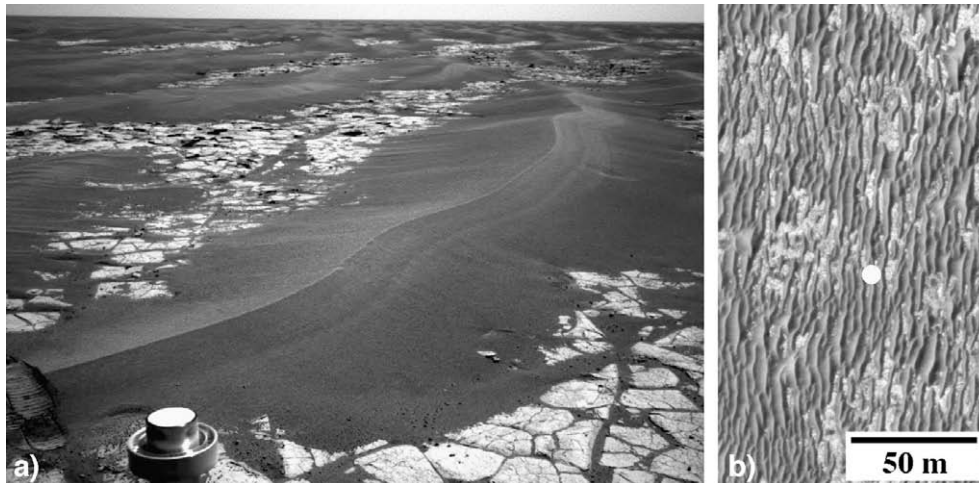


Fig. 1. (a) MER Opportunity NavCam image of large ripples on a fractured bedrock surface, sol 795. (b) Portion of HiRISE image of the Opportunity site (PSP_001414_1780, 25 cm/pixel map projected resolution, NASA/JPL/University of Arizona). White dot indicates the approximate MER location on sol 795.

sand ripples form, there has been general agreement that granule ripples are the result of creep of the large particles induced through the impact of saltating sand grains. The granule-coated surface of sand-cored ripples provides a layer of protection for the underlying sand, allowing the granule-coated ripples to grow in both height and wavelength by causing the impacting saltating grains to hit and rebound off the granules rather than the underlying sand. Trenching in granule ripples indicates that the granules form a monolayer on both flanks of the ripple, but they can be concentrated to thicknesses exceeding 1 cm along the ripple crest, with scattered granules distributed throughout the sand-dominated core of the ripple (Sharp, 1963). Granule ripples have been described in deserts around the world, with reported heights ranging from 1 to 60 cm and wavelengths of <1–25 m (Bagnold, 1941, p. 155; Sharp, 1963; Greeley and Iversen, 1985, pp. 154–155; Fryberger et al., 1992; Jerolmack et al., 2006).

Early spacecraft images of Mars revealed large dune fields, dust mantles of regional extent, and widespread isolated aeolian bedforms on rocky surfaces (e.g., McCauley et al., 1972; Cutts et al., 1977; Greeley et al., 1992). The Mars Orbiter Camera (MOC) revealed in great detail the widespread occurrence of aeolian bedforms across Mars (Malin and Edgett, 2001), later supplemented by the Thermal Emission Imaging System (Hayward et al., 2007) and the High Resolution Imaging Science Experiment (HiRISE; McEwen, 2007). HiRISE is now imaging aeolian features at up to 25 cm/pixel resolution (Bridges et al., 2007). Aeolian bedforms on Mars with wavelengths of 20–80 m, generally oriented transverse to the inferred wind direction, appear to be nearly ubiquitous at equatorial and mid-latitudes (Wilson and Zimbelman, 2004; Balme et al., 2008). Such features, particularly those at the shortest wavelengths, fall within the size range that on Earth is populated by both small sand dunes and large ripples (Wilson, 1972). The long-lived MERs Spirit and Opportunity (Squyres, 2004a,b) have provided conclusive evidence that most of the meter-scale aeolian bedforms at both landing sites are granule ripples (Greeley, 2004, 2006; Sullivan, 2005, 2008). MER results for granule ripples have been compared to analog features at White Sands National Monument (WSNM) in New Mexico, where field studies included documentation of the movement of small (1-cm-high) granule ripples during periods of over an hour in duration (Jerolmack et al., 2006).

Granule ripples are common along the southern margin of the main dune mass at GSDNPP, where we studied them in order to obtain accurate topographic profiles across granule ripples, and in an effort to assess their rate of movement (Zimbelman et al., 2007).

The GSDNPP dune field experiences a bimodal wind regime where the dominant flow is westerly, but with occasional reverse flow from off the Sangre de Cristo Mountains immediately east of the dunes (Merk, 1960; Johnson, 1967; Janke, 2002; Marin et al., 2005; Madole et al., 2008). The sand at GSDNPP has a bimodal particle size distribution, particularly along the southern margin where Medano Creek supplies fresh material (including the granule size fraction) from the nearby mountains (Ahlbrandt, 1979). Several attempts by our group to measure the granule ripple movement over periods of several months proved unsuccessful for a variety of reasons, but during a visit to GSDNPP in the fall of 2006, it became readily apparent that, under the right conditions, the timescale over which granule ripples move can be measured in hours rather than months or years (Zimbelman et al., 2007). The granule ripples examined at GSDNPP are considerably larger than those studied by Jerolmack et al. (2006), but results are quite consistent between both studies, strengthening the credibility of inferences derived from both studies.

3. Documented granule ripple movement at GSDNPP

Two of the authors (JZ and RI) visited GSDNPP on September 15 and 16, 2006, where we used a Trimble R8 Differential Global Positioning System to recover one of our earlier survey lines across granule ripples. More importantly, this visit happened to coincide with the passage of a strong low-pressure area to the north of the park, which resulted in prolonged intense winds from the south–southwest. Wind records from Alamosa airport (located 45 km SSW of the study area), obtained from the National Climatic Data Center (NCDC), quantified the regional wind strength (Fig. 2) and wind direction during our visit, both of which are essentially identical to conditions that we observed locally at the granule ripple site with a hand anemometer and a compass. The airport wind data come from sensors mounted high above the tarmac level (likely well above 1 m height). The NCDC data are recorded every minute using two-minute running averages; they reveal a consistent diurnal pattern in wind intensity, with the strongest winds every afternoon and near-calm conditions every night, during the weeks leading up to the strong wind event.

Winds in south-central Colorado were particularly strong during our visit, at or above the threshold for sand saltation (5 m s^{-1} at 1 m height; Easterbrook, 1969, p. 290) through most of the

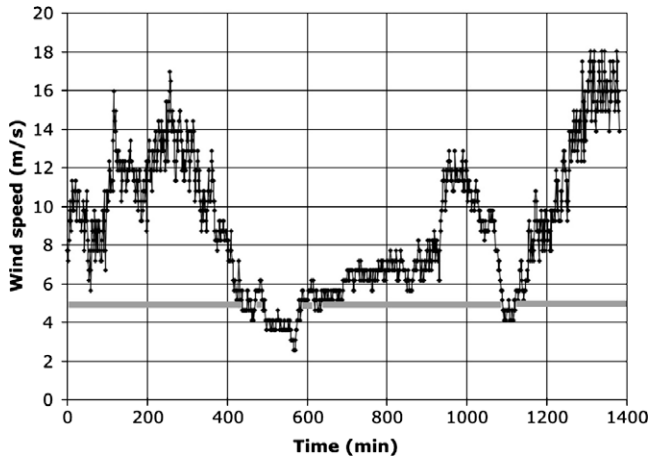


Fig. 2. Wind data for period that flags were in place on granule ripples at GSDNPP. Light grey line indicates 5 m s^{-1} , the saltation threshold wind speed at 1 m height. The ripples shown in Fig. 3 were both flagged at 0 time on the plot. Data are from the Alamosa airport, located 45 km SSW of study site, representative of a height well above 1 m (from NCDC).

night, and well above threshold throughout all of the daylight hours (Fig. 2). The NCDC data documented that the strong winds were consistently from an azimuth of between 190° and 230° (measured clockwise from north) when the wind speed was above threshold. Prior to conducting the survey along the recovered line, one of us (RJ) placed wire flags into the crests of several granule ripples within $\sim 20 \text{ m}$ of the survey line. When the surveying was complete, we were surprised to see that a 3-cm-high granule ripple had clearly moved in less than 2 h (Fig. 3a). A visit to the site the following morning allowed us to document the movement of a nearby 10-cm-high granule ripple over a period of 23 h (Fig. 3b). By September 16, all of the flags on the smaller granule ripples (such as in Fig. 3a) had fallen over due to the complete dispersal of these granule ripples, but the flags remained in place in the larger ripples. Sand-induced failure of two digital cameras resulted in the ripples shown in Fig. 3 being the only ones for which useful rate information could be derived.

4. Results

The surveyed profile across three granule ripples near the location of the flagged ripples was used to obtain accurate shape information for the granule ripples (Fig. 4), which showed that the average stoss slope was 10° and the average lee slope was 7° for ripples $\sim 15 \text{ cm}$ in height; each of the surveyed granule ripples are reasonably symmetrical in shape. Comparison of the September 2006 survey to an April 2006 survey along the same line showed consistent ripple shapes (suggesting continuity during transport), but it was inconclusive for rate constraints due to a lack of information about how many bedforms may have traversed the line between surveys. The time-stamp on the digital images of the flagged granule ripples provided accurate duration information; the 3-cm-high ripple in Fig. 3a moved 2.1 cm in 109 min, and the 10-cm-high ripple in Fig. 3b moved 10.5 cm in 1380 min.

Jerolmack et al. (2006) provide an equation for the creep mass flux (q_c) of ripples, derived from Bagnold's (1941) observations on the rate of dune migration:

$$q_c = (1 - p)\rho cH/2 \quad (1)$$

where p is porosity, ρ is particle density, c is the ripple migration rate, and H is the ripple height. Jerolmack et al. (2006) used their observed average ripple migration rate of 0.04 m h^{-1} ($=1.1 \times 10^{-5} \text{ m s}^{-1}$) obtained from staked 1-cm-high granule ripples, porosity of 0.4, and particle density of 2630 kg m^{-3} to obtain a creep mass flux at WSNM of $9 \times 10^{-5} \text{ kg m}^{-1} \text{ s}^{-1}$ from Eq. (1). If we assume the Jerolmack et al. (2006) particle density and porosity values, then Eq. (1) gives creep mass flux values of 8 and $10 \times 10^{-5} \text{ kg m}^{-1} \text{ s}^{-1}$ for the 3-cm-high and 10-cm-high GSDNPP granule ripples, respectively. We interpret this favorable comparison to indicate that the saltation-induced granule creep flux conditions at GSDNPP and WSNM were quite comparable.

Continuity of shape for the moving GSDNPP granule ripples indicates that the advancing lee side of the ripple sweeps out a parallelogram. The area of this parallelogram is equal to the ripple height times the horizontal length of the crest movement. The parallelogram produced by the advancing ripple lee face can be related to the volume of granules transported over the crest by considering all values to be normalized per unit crest length. The volume estimate assumes that the granules on the advancing lee



Fig. 3. Flagged granule ripple crests, GSDNPP. (a) Photo taken 109 min after flag was placed on crest, indicating 2.1 cm movement (to left) of the 3-cm-high ripple. Smaller granule-coated ripples and sand ripples are in the background. Wind intensity ripped the flag material, which is 6.7 cm along the wire. JRZ, 9/15/06. (b) Photo taken 1380 min after flag was placed on crest (of a different ripple than that shown in (a)), indicating 10.5 cm movement (to right) of the 10-cm-high ripple. Flag material is 6.7 cm along wire. JRZ, 9/16/06.

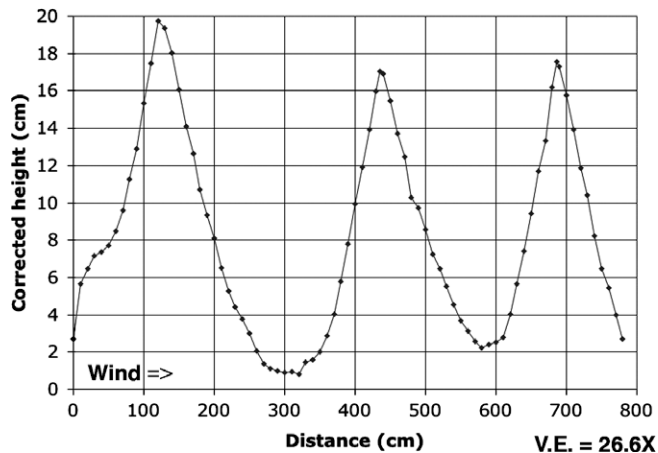


Fig. 4. Topographic profile surveyed across three large granule ripples at GSDNPP (a local slope of 1.5° has been removed). The surveyed ripples are part of an extensive granule ripple field; the surveyed ripples are ~ 20 m WNW of the flagged granule ripples (Fig. 3) along the margin of the granule ripple field. Vertical exaggeration is $26.6\times$.

slope are the primary contributor to the volume of the displaced ripple (i.e. sand that settles between granules can be ignored). The ripple in Fig. 3a then indicates a volume of transported granules of 3 cm (height) times 2.1 cm (crest movement) times 1 cm (per unit crest length) = 6.3 cm^3 , and the ripple in Fig. 3b indicates a transported volume of $10\text{ cm} \times 10.5\text{ cm} \times 1\text{ cm} = 105\text{ cm}^3$. These volumes represent the granules that were transported across each cm of ripple crest in 109 and 1380 min, respectively. The transported volume and duration then give 0.058 cm^3 per minute and 0.076 cm^3 per minute of granules crossing the crest of the ripples shown in Fig. 3a and b, respectively, per cm of crest length.

Granule transport across a ripple crest can be expressed as the number of representative granules moved across a unit crest length per unit time. The granules at GSDNPP are unimodal in size distribution, with a peak abundance (54 wt.%) between the sizes of -0.5 and -0.75 phi, corresponding to diameters of 1.41 to 1.68 mm (from Fig. 22C of Ahlbrandt, 1979). If the granules are considered to be spherical and 1.5 mm in diameter, then a single granule has a volume of $\sim 1.8 \times 10^{-3}\text{ cm}^3$. Longwell et al. (1969, p. 236) gives porosity ranges for sand and gravel as 30–46% and 20–40%, respectively, with median values of 38% for sand and 30% for gravel. If we assume 35% porosity for granule particles, then the volumes determined above translate to 21 and 27 granules per minute crossing each cm of the ripple crest length for the ripples in Fig. 3a and b, respectively. These estimates are consistent with visual observations of tens of granules moving in short hops up the stoss side of a ripple during periods of tens of seconds. The similarity of the two numbers suggests that the sand flux conditions, which moved the granules through impact creep, were comparable over the entire time period represented by the flagged observations, but the potential variability of the wind during the two periods of observation should be evaluated.

The NCDC wind data (Fig. 2) corresponds to the total time period covered by the two flagged ripples (both crests were flagged at time = 0). It does not seem reasonable to use these wind data for detailed flux calculations at GSDNPP since they represent the wind at a site 45 km from the granule ripple location. However, a general assessment can be made of wind strength during the two periods covered by the photographed ripples. The NCDC wind strength values were summed over both periods and divided by the duration, giving average wind speeds during the two periods of observation of 9.3 and 8.9 m s^{-1} (for a height well above 1 m) for the 109 and 1380 min durations covered by the ripples in Fig. 3a and 3b,

respectively. While this result cannot be taken to indicate equivalent sand flux conditions throughout the entire duration of both time periods, the comparable average wind speeds for both periods is supportive of the similar volumes and numbers of granules moved during both periods. Both documented ripples are therefore indicative of ~ 24 granules per minute (per cm crest length) being driven across the ripple crest by wind that averaged $\sim 9\text{ m s}^{-1}$ (at a height well above 1 m), which is ~ 1.8 times the saltation threshold wind speed for sand. Sediment transport rates scale non-linearly with fluid velocity, but with only two observation points, use of the average number of granules moved across both ripple crests seems preferable to trying to estimate a meaningful standard deviation. The value of 24 granules per minute crossing each cm of ripple crest also can be expressed in units equivalent to the creep mass flux (Eq. (1)) by assuming spherical granules 1.5 mm in diameter and the Jerolmack et al. (2006) particle density, which gives a mass flux of $1.9 \times 10^{-4}\text{ kg m}^{-1}\text{ s}^{-1}$, within a factor of two of the creep mass flux calculated above.

5. Application to Mars

The Opportunity rover on Mars observed many large ripples on the plains of Meridiani Planum (see Fig. 1), with Microscopic Imager evidence that most of the large ripples are coated with hematite-enriched 1–2 mm particles (Sullivan, 2005; Weitz et al., 2006). Stereo Panoramic Camera images from Opportunity on sol 794 (in the immediate vicinity of the ripples shown in Fig. 1) provided measurements of a typical ripple height of ~ 25 cm, and ripple surface slopes of ~ 5 – 10° , comparable to the slopes measured on large granule ripples at GSDNPP (Fig. 4). The GSDNPP results for granule ripple movement can be related to potential granule ripple movement on Mars through consideration of the differing conditions on the two planets. Atmospheric density, acceleration of gravity, and friction speed (or shear velocity) on Earth and Mars differ by factors of 79, 2.7, and 0.14 (for threshold friction speed), respectively, expressed as Earth values divided by Mars values; values for atmospheric density and acceleration of gravity are from Ladders and Fegley (1998, pp. 128, 160, 190, 192), and threshold friction speed are from Greeley and Iversen (1985, p. 53). Sand flux is directly proportional to both atmospheric density and the cube of the friction speed, and it is inversely proportional to the acceleration of gravity (Bagnold, 1941, p. 66). Consequently, sand flux on Mars should be $\sim 12\times$ the sand flux on Earth once saltation commences. The GSDNPP granule movement rate then translates to ~ 290 granules per minute (per cm crest length) across the ripple crest under continuous wind above threshold. Almedia et al. (2008) recently derived threshold friction speeds for Earth and Mars of 0.26 and 1.12 m s^{-1} , respectively, through directly solving the motion of particles through a fully developed turbulent wind field; the ratio of these fully turbulent threshold friction speeds is 0.23, which results in a sand flux on Mars $\sim 2.6\times$ the sand flux on Earth once saltation commences. The GSDNPP granule movement rate then corresponds to ~ 63 granules per minute (per cm crest length) on Mars using the Almedia et al. (2008) threshold friction speed values.

The derived granule movement rate for Mars can be used to estimate how long it could take to produce movement of a granule ripple on Mars. For a 25-cm-tall granule-coated ripple like those seen at Meridiani Planum, if the ripple crest moved 1 cm, then 25 cm^3 of granules moved across each centimeter of the crest. For 1.5-mm-diameter spherical granules and 35% porosity (as was assumed for the GSDNPP calculation), this volume corresponds to ~ 9000 granules moved across each centimeter of crest length. The Mars granule rate derived above indicates that transport of 9000 granules across each centimeter of the ripple crest

would require from ~ 31 min (Greeley–Iversen threshold friction speeds) to ~ 142 min (Almeida et al. threshold friction speeds) of continuous saltation-inducing wind to produce 1 cm of ripple movement.

Wind conditions required for continuous saltation over time intervals of tens to hundreds of minutes are exceedingly unlikely for the present martian atmosphere. Saltation transport on Mars occurs only very occasionally; intervals between saltation events at the Viking Lander sites were estimated to be on the order of 5 Earth-years, with each gust of saltation lasting on the order of 40 s (Arvidson et al., 1983; Moore, 1985; as cited by Almeida et al., 2008). Almeida et al. (2008) used these Viking Lander observational constraints to estimate that the fraction of time during which saltation transport occurs on Mars under present conditions is $\sim 2.5 \times 10^{-7}$. This small saltation frequency then indicates that 1 cm of movement for a 25-cm-high granule ripple could require from $\sim 7.4 \times 10^9$ s = 240 Earth-years (Greeley–Iversen) to $\sim 7.0 \times 10^{10}$ s = 2200 Earth-years (Almeida). Clearly these estimates suggest that the martian granule ripples would be long-lived features under conditions typical of the Viking lander sites. This inference is consistent with observations of old ejecta blocks partly embedded into Meridiani Planum granule ripples that have been eroded down to conform with ripple surfaces before the granule ripples have moved on (Sullivan et al., 2007).

What wind speeds on Mars are comparable to the conditions at GSDNPP when the granule ripple movement was observed? Sullivan (2005) estimated that, at the Opportunity site, recent winds activated basaltic sand caught in temporary particle traps (e.g., small craters) when $u_t^* \sim 2$ m/s (the threshold wind friction speed), which corresponds to a wind speed of ~ 45 m s $^{-1}$ at 1 m height. Sullivan (2005) concluded that such winds probably moved 1- to 2-mm-diameter hematite fragments through impact creep driven by the saltating sand, consistent with the inferences made by Jerolmack et al. (2006). If 45 m s $^{-1}$ at 1 m height is taken to be the local threshold for saltation at the Opportunity site, then the GSDNPP conditions (~ 1.8 times the saltation threshold wind speed) suggest that an average wind speed of ~ 80 m s $^{-1}$ at 1 m height may be comparable at the Opportunity site to the situation when granule ripple movement was observed at GSDNPP, a value significantly higher than any wind gust observed at the Viking landing sites over periods of 4–6 years (e.g., Arvidson et al., 1983; Moore, 1985).

Martian granule ripples possibly could represent paleoclimatic conditions substantially different from that of the current martian atmosphere (e.g., the atmosphere may have been denser than it is today at intervals during the Late Amazonian Epoch; Laskar et al., 2004). However, 1–2 mm concretions were observed to be common within the bedrock to the south of the Eagle–Endurance area (Weitz et al., 2006), effectively removing any need to invoke stronger winds ($u_t^* > 3$ m/s) to sort granule-sized particles (through saltation of the concretions) to generate the observed narrow distribution of size fractions (e.g., Sullivan, 2005; Jerolmack et al., 2006). Granule movement through impact creep alone now appears to be sufficient to explain the observed particle size distributions on the surface of martian granule ripples (e.g., Weitz et al., 2006).

6. Conclusions

Granule ripples are prevalent on both Earth and Mars where sand, granule-sized particles, and wind are abundant. Granule creep produced by the impact of saltating sand caused observable movement of granule ripples at GSDNPP during a particularly strong wind event in the fall of 2006. The documented movement of two GSDNPP granule ripples indicates that ~ 24 granules per minute (per cm crest length) were driven across the ripple crest

by wind averaging ~ 9 m s $^{-1}$ (at a height well above 1 m), which well exceeds the sand saltation threshold wind speed. The rate of movement of the GSDNPP granule ripples suggests that comparable granule ripples on Mars likely would require from hundreds to thousands of Earth-years to produce discernable movement under current martian atmospheric conditions.

Acknowledgments

The comments of Nathan Bridges and an anonymous reviewer were extremely helpful in correcting and clarifying earlier versions of the manuscript. We are grateful for the support of personnel from both the Great Sand Dunes National Park and Preserve and the National Climatic Data Center. This work was supported in part by research grant NNG04GN88G from the Mars Data Analysis Program of NASA.

References

- Ahlbrandt, T.S., 1979. Textural parameters of eolian deposits. In: McKee, E.D. (Ed.), *A Study of Global Sand Seas*, U.S. Geol. Survey Prof. Pap. 1052, U.S. Gov. Printing Office, Washington, DC, pp. 21–51.
- Almeida, M.P., Parteli, E.J.R., Andrade, J.S., Hermann, H.J., 2008. Giant saltation on Mars. *Proc. Nat. Acad. Sci.* 105 (17), 6222–6226. doi:10.1073/pnas.0800202105.
- Anderson, R.S., 1987. A theoretical model for aeolian impact ripples. *Sedimentology* 34, 943–956.
- Anderson, R.S., Haff, P.K., 1988. Simulation of eolian saltation. *Science* 241, 820–823.
- Anderson, R.S., Haff, P.K., 1991. Wind modification and bed response during saltation of sand in air. *Acta Mech.* 1 (Suppl.), 21–51.
- Anderson, R.S., Bunas, K.L., 1993. Grain size segregation and stratigraphy in aeolian ripples modeled with a cellular automaton. *Nature* 365, 740–743.
- Arvidson, R.E., Guinness, E.A., Moore, H.J., Tillman, J., Wall, S.D., 1983. Three Mars years: Viking Lander 1 imaging observations. *Science* 222, 463–468.
- Bagnold, R.A., 1941. *The Physics of Blown Sand and Desert Dunes*. Chapman and Hall, London.
- Balme, M., Berman, D.C., Bourke, M.C., Zimelman, J.R., 2008. Transverse Aeolian Ridges (TARs) on Mars. *Geomorphology* 101, 703–720. doi:10.1016/j.geomorph.2008.03.011.
- Bridges, N.T., Beissler, P.E., McEwen, A.S., Thomson, B.J., Chuang, F.C., Kerkenhoff, K.E., Keszthelyi, L.P., Martinez-Alonso, S., 2007. Windy Mars: A dynamic planet as seen by the HiRISE camera. *Geophys. Res. Lett.* 34, L23205. doi:10.1029/2007GL031445.
- Cutts, J.A., Blasius, K.R., Briggs, G.A., Carr, M.H., Greeley, R., Masursky, H., 1977. North polar region of Mars: Imaging results from Viking 2. *Science* 194, 1329–1337.
- Easterbrook, D.J., 1969. *Principles of Geomorphology*. McGraw-Hill Book Co., New York.
- Ellwood, J.M., Evans, P.D., Wilson, I.G., 1975. Small scale aeolian bedforms. *J. Sed. Petrol.* 45, 554–561.
- Fryberger, S.G., Hesp, P., Hastings, K., 1992. Aeolian granule ripple deposits. *Namibia. Sed.* 39, 319–331.
- Greeley, R., Iversen, J.D., 1985. *Wind as a Geological Process on Earth, Mars, Venus, and Titan*. Cambridge University Press, New York.
- Greeley, R., Lancaster, N., Lee, S., Thomas, P., 1992. Martian aeolian processes, sediments, and features. In: Kieffer, H.H., Jakosky, B.M., Snyder, C.W., Matthews, M.S. (Eds.), *Mars*. University of Arizona Press, Tucson, pp. 730–766.
- Greeley, R. and 27 colleagues, 2004. Wind-related processes detected by the Spirit rover at Gusev crater, Mars. *Science* 305, 810–821.
- Greeley, R. and 21 colleagues, 2006. Gusev crater: Wind-related features and processes observed by the Mars Exploration Rover Spirit. *Mars. J. Geophys. Res.* 111, E02S09. doi:10.1029/2005JE002491.
- Hayward, R.K., Mullins, K.F., Fenton, L.K., Hare, T.M., Titus, T.N., Bourke, M.C., Colprete, A., Christensen, P.R., 2007. Mars Global Digital Dune Database and initial science results. *J. Geophys. Res.* 112, E11007. doi:10.1029/2007JE002943.
- Janke, J.R., 2002. An analysis of the current stability of the dune field at Great Sand Dunes National Monument using temporal TM imagery (1984–1998). *Rem. Sens. Environ.* 83, 488–497.
- Jerolmack, D.J., Mohrig, D., Grotzinger, J.P., Fike, D.A., Watters, W.A., 2006. Spatial grain size sorting in eolian ripples and estimation of wind conditions on planetary surfaces: Application to Meridiani Planum, Mars. *J. Geophys. Res.* 111, E12S02. doi:10.1029/2005JE002544.
- Johnson, R.B., 1967. *The Great Sand Dunes of Southern Colorado*. U.S. Geol. Survey Prof. Pap. 575C, U.S. Gov. Printing Office, Washington, DC, pp. 177–183.
- Laskar, J., Correia, A., Gastineau, F., Joutel, F., Levrard, B., Robutel, P., 2004. Long term evolution and chaotic diffusion of the insolation quantities of Mars. *Icarus* 170, 343–364.
- Lodders, K., Fegley, B., 1998. *The Planetary Scientist's Companion*. Oxford University Press, New York.

- Longwell, C.R., Flint, R.F., Sanders, J.E., 1969. *Physical Geology*. John Wiley & Sons, New York. 685 p.
- Madole, R.F., Roming, J.H., Aleinikoff, J.N., VanSistine, D.P., Yacob, E.Y., 2008. On the origin and age of the Great Sand Dunes, Colorado. *Geomorphology* 99, 99–119. doi:10.1016/j.geomorph.2007.10.006.
- Malin, M.C., Edgett, K.S., 2001. Mars Global Surveyor Mars Orbiter Camera: Interplanetary cruise through primary mission. *J. Geophys. Res.* 106, 23429–23570.
- Marin, L., Forman, S.L., Valdez, A., Bunch, F., 2005. Twentieth century dune migration at the Great Sand Dunes National Park and Preserve, Colorado: Relation to drought variability. *Geomorphology* 70, 163–183.
- McCaughey, J.F., Carr, M.H., Cutts, J.A., Hartmann, W.K., Masursky, H., Milton, D.J., Sharp, R.P., Wilhelms, D.E., 1972. Preliminary Mariner 9 report on the geology of Mars. *Icarus* 17, 289–327.
- McEwen, A.S. and 14 colleagues, 2007. Mars Reconnaissance Orbiter's High Resolution Imaging Science Experiment (HiRISE). *J. Geophys. Res.* 112, E05S02. doi:10.1029/2005JE002605.
- Merk, G.P., 1960. Great sand dunes of Colorado. In: *Guide to the Geology of Colorado*, Geol. Soc. Am. Rocky Mtn. Assoc. Geol. Col. Sci. Soc., Denver, pp. 127–129.
- Moore, H.J., 1985. The martian dust storm of sol 1742. *J. Geophys. Res.* 90, 163–174.
- Sharp, R.P., 1963. Wind ripples. *J. Geol.* 71, 617–636.
- Squyres, S.W. and 49 colleagues, 2004a. The Spirit rover's Athena science investigation at Gusev crater, Mars. *Science* 305, 794–799.
- Squyres, S.W. and 50 colleagues, 2004b. The Opportunity rover's Athena science investigation at Meridiani Planum, Mars. *Science* 306, 1698–1703.
- Sullivan, R. and 17 colleagues, 2005. Aeolian processes at the Mars Exploration Rover Meridiani Planum landing site. *Nature* 436. doi:10.1038/nature03641.
- Sullivan, R., Arvidson, R., Grotzinger, J., Knoll, A., Golombek, M., Jolliff, B., Squyres, S., Weitz, C., 2007. Aeolian geomorphology with MER Opportunity at Meridiani Planum, Mars. *Lunar Planet. Sci.* XXXVIII, Abstrat #2048, Lunar Planet. Inst., Houston.
- Sullivan, R. and 10 colleagues, 2008. Wind-driven particle mobility on Mars: Insights from Mars Exploration Rover observations at "El Dorado" and surroundings at Gusev Crater. *J. Geophys. Res.* 113, E06S07. doi:10.1029/2008JE003101.
- Weitz, C.M., Anderson, R.C., Bell, J.F., Farrand, W.H., Herkenhoff, K.E., Johnson, J.R., Jolliff, B.L., Morris, R.V., Squyres, S.W., Sullivan, R.J., 2006. Soil grain analyses at Meridiani Planum, Mars. *J. Geophys. Res.* 111, E12S04. doi:10.1029/2005JE002541.
- Wilson, I.G., 1972. Aeolian bedforms: Their development and origins. *Sedimentology* 19, 173–210.
- Wilson, S.A., Zimbelman, J.R., 2004. Latitude-dependent nature and physical characteristics of transverse aeolian ridges on Mars. *J. Geophys. Res.* 109, E10003. doi:10.1029/2004JE002247.
- Zimbelman, J.R., Irwin III, R.P., Williams, S.H., Bunch, F., Valdez, A., Stevens, S., 2007. Granule ripples on Earth and Mars: Documented movement at Great Sand Dunes National Park, and implications for granule movement on Mars. *Lunar Planet. Sci.* XXXVIII. Abstract #1324. Lunar Planet. Sci., Houston.